ARTICLE

Passive Control of Base Pressure in a Converging-Diverging Nozzle with Area Ratio 2.56 at Mach 1.8

Nur Husnina Muhamad Zuraidi[1], Sher Afghan Khan[1,*], Abdul Aabid[2,*], Muneer Baig[2] and Istiyaq Mudassir Shaiq[3]

[1]Department of Mechanical Engineering, International Islamic University Malaysia, P.O. Box 10, Kuala Lumpur, 50728, Malaysia

[2]Department of Engineering Management, College of Engineering, Prince Sultan University, P.O. Box 66833, Riyadh, 11586, Saudi Arabia

[3]School of Aerospace Engineering, Engineering Campus, Universiti Sains Malaysia, Nibong Tebal, Pulau Pinang, 14300, Malaysia

*Corresponding Authors: Sher Afghan Khan. Email: sakhan@iium.edu.my; Abdul Aabid. Email: aaabid@psu.edu.sa

ABSTRACT

In this study, a duct is considered and special attention is paid to a passive method for the control of the base pressure relying on the use of a cavity with a variable aspect ratio. The Mach number considered is 1.8, and the area ratio of the duct is 2.56. In particular, two cavities are examined, their sizes being 3:3 and 6:3. The used L/D spans the interval 1–10 while the NPRs (nozzle pressure ratio) range from 2 to 9. The results show that the control becomes effective once the nozzles are correctly expanded or under-expanded. The pressure contours at different NPR and L/D are presented. It is shown that the NPR and cavity location strongly influence the base pressure. The NPR, Mach number, and cavity aspect ratio have a strong effect on the base pressure in the wake region.

KEYWORDS

Base pressure; passive control; computational fluid dynamics (CFD); supersonic; aerodynamics; cavity

1 Introduction

Baseflow studies at high Mach numbers continue to be an area of research because of their many different applications in the aerospace industry, defence, and space research. The flow field at a blunt base is characterized by flow separation, and reattachment can be divided into two regions: the central and the separated regions. The shear layer will generate strong vortices in the wake region, increasing the overall drag force. The net drag force comprises skin friction, wave, and base drag for any aerodynamic body. For the Mach number, less than unity total drag will consist of skin friction drag and base drag. However, wave drag will be an additional component at sonic and supersonic Mach numbers. The literature review reveals that the base drag component is two-thirds of the total drag in transonic speed.

There are two primary techniques for base drag control; one is active, and the other is passive. In the case of dynamic control, an additional energy source is needed. In the case of passive flow, control is accomplished through the geometrical change in the flow field. Active control can be switched on or off as required, as well as when required. Dynamic flow control management is more beneficial than passive

control but demands additional effort and expense. Actuators are at the heart of implementing active flow control and have traditionally been the weakest link in inflow control technology development. However, passive management requires no external power source. Passive control using splitter plates, ribs, cavities, boat tailing, etc., are used as control mechanisms; it only needs to change the geometry at the enlarged duct. Passive control devices are always in operation, regardless of need or performance penalty.

Hence this study aims to regulate the base pressure through passive control through a cavity of different aspect ratios. Because any increase in base pressure, and consequently any decrease in base pressure, will result in a considerable fluctuation in the range of projectiles. The primary focus is the passive control technique. The function of passive control is to disrupt the base flow field. The geometry of the passive control must be optimized to manipulate passive control. The primary focus is the passive control technique in the form of a cavity. The cavities' function is to control base pressure. This study attempts to study the effect of the cavity location and its geometry on base pressure at supersonic Mach number.

The rough surfaces will have higher skin friction than smooth surfaces. Second, the base drag is a drag induced by the negative pressure originating behind a projectile base. It persists because of the influence of the upstream boundary layer. Third, the drag caused by the formation of shocks at supersonic and high supersonic speeds is referred to as wave drag [1]. First, the flow past a projectile is an example of external flow. Second, the internal flow is the flow in the pipe that is entirely bounded by solid surfaces. Wick [2] explained internal flow passed from a nozzle to a duct with a sudden increase in area. First, the flow is affected upstream. When the flow at the entry is sonic or supersonic, the flow will be affected by the entrance. But when it is subsonic, the flow will be affected by the flow past an inlet. Second is the pressure at the corner, which is determined by upstream conditions when the flow in the entrance section is sonic or supersonic.

2 Literature Review

This section has provided the work done by the researcher in fluid dynamics studies and high-speed flow control. For the first, we have observed that the effect of the boundary layer on sonic flow through an abrupt change in the cross-sectional area was studied by Wick [2]. He considered the boundary layer a fluid source for the corner flow and an insulating layer that reduced the jet's pumping efficiency. He also finds the base corner as the summation of two mass supplies consisting of the boundary layer flow around the corner and the backflow in the boundary layer along the expanded section. Therefore, the pressure in the expansion corner is related to the boundary layer type and the thickness upstream of the area growth. The supersonic flow exiting from a CD nozzle can be any of the three conditions; over-expanded, under-expanded, and ideally expanded. The flow from the supersonic nozzle is said to be ideally expanded when the flow Pe/Pa $= 1$ at design conditions. The flow is over-expanded when the pressure ratio Pe/Pa < 1. However, the flow is under-expanded when the pressure ratio Pe/Pa > 1. Pandey et al. [3] studied the nozzle flow in the over-expanded and under-expanded cases at supersonic Mach numbers. An expansion fan is located at the nozzle exit for under-expanded flow. There will be an oblique shock wave at the nozzle exit in the case of the overexpanded nozzle. Consequently, the reattachment length will vary in both cases. The vortices formed inside the region between the base and the reattachment point will create suction. The suction strength depends on the reattachment length, NPR, and Mach number.

Nusselt [4] was the first to conduct tests with the high-velocity gas flow with sudden expansion. He concluded that if the entrance velocity is subsonic, the base pressure is the same as the entrance pressure. If the entrance flow is supersonic, the base pressure could be equal to, less than, or greater than the entrance pressure. When the entrance Mach number is unity, no jet region is affected by the expansion waves from the opposite corner. Korst [5] investigated the base pressure in a transonic and supersonic flow where the flow entering the base after the wake is sonic or supersonic. He devised a theoretical

model based on free stream and mass conservation in the separated region. He also studied the effect of mass bleed in the wake region. Thus, the results obtained agreed closely with Wick's results.

The study's findings on base pressure and noise caused by air expanding suddenly in a cylindrical duct were reported by Anderson et al. [6]. First, the minimum base pressure value depends on the duct-to-nozzle area ratio and the nozzle geometry. Second, the overall noise is a minimum at jet pressure approximately equal to that required to produce minimum base pressure. Overall noise is minimum at jet pressure, roughly equivalent to that needed to make minimum base pressure. Srikanth et al. [7] studied the airflow from a plenum chamber that suddenly expanded to a constant circular cross-sectional area tube. They varied NPR from 1.1 to 3.0, the L/D ratio was between 1 to 10, and the area ratio ranged from 2.78 to 8.38. Their study revealed that the base pressure depends on the expansion area ratios, the overall pressure ratios, and the duct L/D ratios. The separation and reattachment length depends on the area ratio of the inlet enlargement. The duct length must exceed a definite minimum value for minimum base pressure. Asadullah et al. [8] stated that flow complexity makes it necessary to understand the method within and around it and its effects on base pressure which requires a multidisciplinary approach. This concept creates a convenient pressure gradient when two counter-rotating vortices inside the cavities are trapped. These trapped vortices over the suction surface will ensure a different low-pressure region and produce less drag. The presence of cavities increased the lift-to-drag ratio.

The base cavity at angles of incidence varied from 0° to 25° studied by Tanner [9]. Based on the experiment, the results gathered for the base cavity at angles of incidence influenced by tail surfaces on base pressure. He concluded that the base pressure coefficient for the cavity base is higher than that for the base without a cavity. Thus, the base pressure coefficient for the cavity base is more significant than without the cavity base. Tanner [9] stated that cavity depths influence the base pressure at zero angle incidence. The greater the base cavity depths, the lower the value of the base pressure coefficient. As a result, a base cavity in axisymmetric flow could increase base pressure while decreasing base drag (Fig. 1).
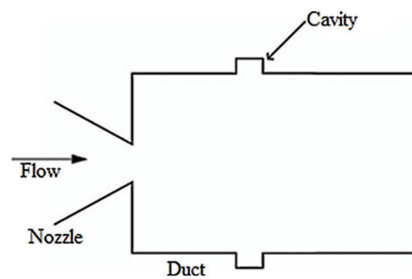
Figure 1: Cavities in enlarged duct [9]

Viswanath et al. [10] investigated the effectiveness of passive devices for axisymmetric base drag reduction at Mach 2. The wake behind a blunt base is nearly constant at supersonic speeds. The vortex locking mechanism is designed to impact drag by preventing vortex shedding positively. They studied the efficiency of devices that can modify the base pressure by affecting the mean flow in the wake region. As a result, ventilated cavities offered significant base-drag reduction. There has been a 50% rise in base pressure. Furthermore, based on Schlieren's photographs, the bleed effect causes the free shear layers to shift outward to accommodate the higher base pressure, reducing the shoulder expansion fan and the recompression waves. Viswanath [11] researched about flow characteristics of a multi-step after-body which is shown in Fig. 2. In general, afterbody boat-tailing can lead to a decrease in drag. At Mach 2, the flow past a multi-step afterbody was chosen, influencing the separated flow at the steps and base pressure. Boundary layer separation-reattachment processes influenced base flow resulting in distortion in the

turbulent boundary layer. The length to height ratio of the step influenced the recovery of a boundary layer that will contribute to reattachment and separation conditions. One of the efficient methods to reduce the base drag of blunt bases is afterbody boat-tailing.
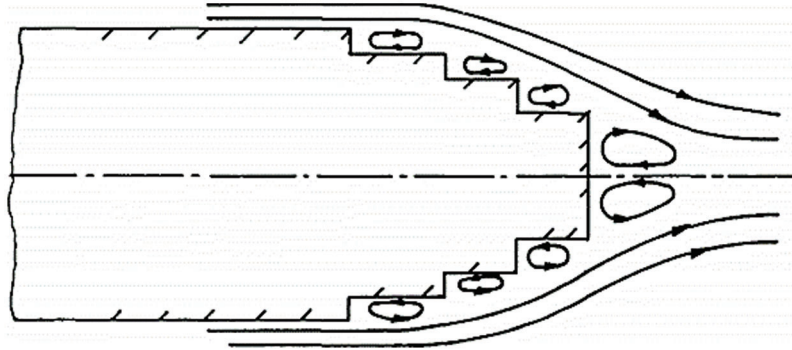
Figure 2: Sketch of a multi-step afterbody [11]

Viswanath [12] stated that a disc regulates the flow downstream of a blunt base, resulting in a smooth flow in the wake zone with a vortex between the recirculation region and the disc. Furthermore, the drag will be affected by the shape of the disc's rim. The drag reduction for typically locked vortex at low Mach numbers was demonstrated by Mair [13]. Owing to the precarious nature of the wake flow, he revealed that the body-disc configuration could experience a spike in the resistance for a specific pattern of disc diameter. This situation is caused by an erratic vortex confined within the base and the disc. A splitter plate is a component that directs the boundary layer away from the engine intake. Rathakrishnan [14] examined the impact of the splitter plate on the blunt body, which divides the flow in the front and at the base to regulate drag. A backplate causes the base pressure to increase slightly compared to a forward plate for a plate at the center. Since the splitter plate divides the wake and prevents the development of powerful eddies at the base, it can also be seen that $l/h > 1$ is the most effective in lowering the base pressure coefficient than $l/h < 1$. According to Radhakrishnan [15], circulation in the duct reduces the flow's oscillations. The flow will grow efficiently at the base. As a result, passive flow management in annular ribs will significantly reduce base pressure compared to plain passage for aspect ratio. The base pressure is minimum when the annular rib's aspect ratio is 3:1. Ribs will increase the base pressure with aspect ratios of 3:2 and 3:3 due to the increased rib height. Increased height will generate secondary vortices and arrest the reverse flow towards the recirculation zone.

In recent work, several studies have been found in the literature in which the researchers utilized the active microjet controller to control the supersonic flows in a sudden expansion duct of a CD nozzle by using an experimental approach [16–19]. Additionally, a two-dimensional Ansys model has been designed and appropriate boundary conditions were applied for the simulation and validated with experimental results [20–22]. To avoid more experimentation and save cost and energy optimization techniques were used and predicted the optimal results of flow control using the techniques like the design of experiments [19,23] and [24], and machine learning [25]. In all techniques, it has successfully presented the flow control problems and proved an effective approach [26].

After doing exhaustive literature work, we have found that in the last four decades, many studies have been reported on inflow control, either high speed or low speed, using experimental and CFD methods. In contrast, only a few studies were found in a high-speed control in which CD nozzle with sudden expansion. Specifically, with a cavity, the literation shows only a few studies, based on the experimental work.

Therefore, this research aims to reproduce/validate the Raymer [1] work using the advanced soft computing tool ANSYS fluent-based CFD.

3 Governing Equations

The complete set of governing equations in terms of continuity, momentum, and energy can be written for compressible ideal gas flow as follows and the parameters with a bar reflect the time-averaged values [27,28],

$$\frac{\partial}{\partial t} + \frac{\partial}{\partial x_i} (\bar{\rho} \widetilde{u}_i) = 0 \tag{1}$$

$$\frac{\partial}{\partial t} (\bar{\rho} \widetilde{u}_i) + \frac{\partial}{\partial x_j} (\bar{\rho} \widetilde{u}_j \widetilde{u}_i) = -\frac{\partial \bar{p}}{\partial x_i} + \frac{\partial}{\partial x_j} \left(\widetilde{\sigma}_{ij} - \overline{\rho u_i'' u_j''} \right) \tag{2}$$

$$\frac{\partial}{\partial t} \left(\bar{\rho} \widetilde{E} \right) + \frac{\partial}{\partial x_j} \left[\bar{\rho} \widetilde{u}_j \left(\widetilde{E} + \bar{p} \right) \right] = \frac{\partial}{\partial x_j} \left[\widetilde{u}_i \left(\widetilde{\sigma}_{ij} - \overline{\rho u_i'' u_j''} \right) \right] - \frac{\partial}{\partial x_j} \widetilde{q}_j + \frac{\partial}{\partial x_j} \left[-c_p \overline{\rho u_j'' T''} + \overline{u_i'' \sigma_{ij}} - \overline{\rho u_j'' \frac{1}{2} u_i'' u_i''} \right] \tag{3}$$

where,

$\bar{\rho}$ = Density

$\widetilde{u}_i$ = Turbulence Velocity

$\bar{p}$ = Pressure

$\widetilde{E}$ = Energy

For the compressible flow analysis, the density of a gas is a variable. So, the ideal gas constant is selected. The third assumption is that velocity flow is considered turbulent flow. Turbulence happens when there is the existence of random fluctuations in the fluid. Hence, the k-epsilon $(k - \varepsilon)$ turbulence model is used. This model provides economy, sturdiness, and adequate precision for flow conditions. The turbulent kinetic energy (k equation) can be described as:

$$\frac{\partial(\rho u K)}{\partial z} + \frac{1}{r} \frac{\partial(\rho v K)}{\partial r} \frac{\partial}{\partial z} \left[\left(\mu + \frac{\mu_t}{\sigma_k} \right) \frac{\partial K}{\partial z} \right] + \frac{1}{r} \frac{\partial}{\partial r} \left[r \left(\mu + \frac{\mu_t}{\sigma_k} \right) \frac{\partial K}{\partial r} \right] \rho \varepsilon + G \tag{4}$$

where, σ_k is the turbulent Prandtl number for K, ε is the turbulent kinetic energy dissipation rate and G is the turbulence generation term. G can be written as:

$$G = \mu_t \left(\frac{\partial u_i}{\partial x_j} + \frac{\partial u_j}{\partial x_i} \right) \frac{\partial u_i}{\partial x_j} - \frac{2}{3} k \delta_{ij} \frac{\partial u_i}{\partial x_j} \tag{5}$$

The kinetic energy of turbulence dissipation (ε equation) can be described as:

$$\frac{\partial(\rho u \varepsilon)}{\partial z} + \frac{1}{r} \frac{\partial(\rho v \varepsilon)}{\partial r} = \frac{\partial}{\partial z} \left[\left(\mu + \frac{\mu_t}{\sigma_\varepsilon} \right) \frac{\partial \varepsilon}{\partial z} \right] + \frac{1}{r} \frac{\partial}{\partial r} \left[r \left(\mu + \frac{\mu_t}{\sigma_\varepsilon} \right) \frac{\partial \varepsilon}{\partial r} \right] - C_1 f_1 \left(\frac{\varepsilon}{K} \right) G - C_2 f_2 \left(\frac{\varepsilon^2}{K} \right) \tag{6}$$

where, μ_t is the turbulent viscosity, $C_1, C_2, f_1, f_2, \sigma_\varepsilon$ and μ_t are arbitrary constants for the kinetic energy of turbulence dissipation model in Eqs. (6) and (7). The fourth assumption is that fluid viscosity is a function of temperature. The law of Sutherland was chosen as the dynamic viscosity. Sutherland's viscosity model based on three coefficients is defined as:

$$\mu = \mu_0 \left(\frac{T}{T_0}\right)^{3/2} \frac{T_0 + S}{T + S} \tag{7}$$

where, μ is the viscosity, μ_0 is the reference viscosity, T is static temperature, T_0 is the reference temperature and S is the Sutherland constant. The last assumption is the flow exits from the duct at ambient atmospheric pressure.

4 Finite Volume Method

To perform the finite volume method (FVM) Ansys commercial software was used for the entire process with ANSYS Workbench, based on Fluid Flow (Fluent) analysis systems. Fig. 3 depicts an axisymmetric convergent-divergent nozzle model connected to a concentrated axisymmetric duct with annular rectangular cavities. The dimensions for the convergent-divergent nozzle with suddenly expanded circular are based on an experimental setup by Raymer [1].
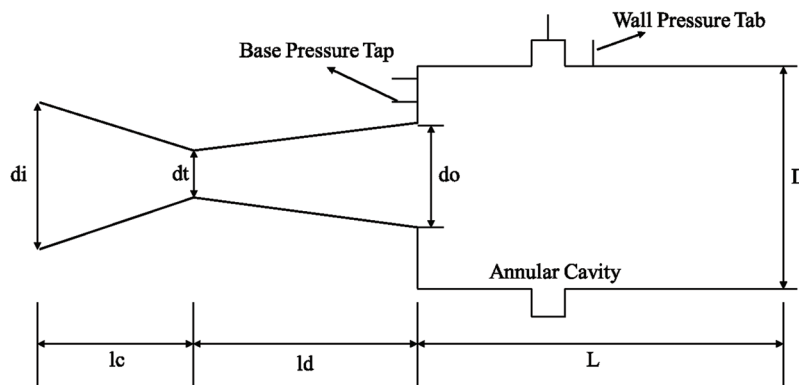
Figure 3: Converging diverging nozzle model suddenly expanded into a duct with an annular cavity [1]

The Mach number for the present work is 1.8. The duct diameter is fixed to D = 16 mm and the duct length, L, varies based on the L/D ratio. The nozzle inlet is 22.34 mm in diameter, and the nozzle outlet is 10 mm in diameter. The convergent angle, θ_c is 15°, and the divergent angle, θ_d is 5°. In this study, two-cavity aspect ratios were used. The aspect ratio is defined as the ratio w/h. The dimension for the cavity aspect ratio 1 is 3:3, and the size for the cavity aspect ratio 2 is 6:3. The duct length, L, varies with the L/D ratio, ranging from 1 to 10.

The next critical step is mesh generation after creating the domain geometry with the Design Modeler of fluent software, as shown in Fig. 4. The domain geometry is divided into smaller sub-domain. The essential fluid flows are numerically solved according to each mesh of cells in the domain geometry to determine the discrete values of flow properties such as velocity and pressure. As per Koomullil et al. [29], mesh generation can be divided into two types built on the network topology of the elements which fill the domain: structured meshes and unstructured meshes. The mesh is generated automatically using the Quadrilateral Dominant method in this project. This method ensures that the element's size is symmetrical throughout the geometry.
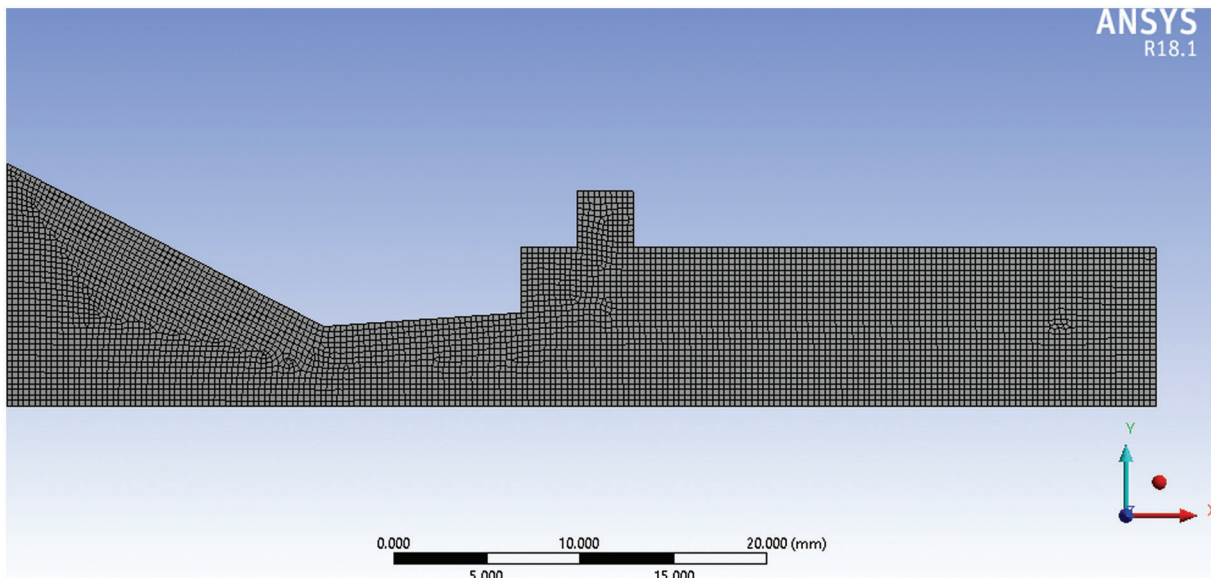
Figure 4: 2D ANSYS fluent symmetry model of converging diverging nozzle

For boundary conditions, flow is assumed compressible and involves heat transfer; the energy equation was chosen. Then, the other assumption stated that velocity turbulent is considered turbulent flow. So, the k-epsilon (2 equation) model was selected. The k-epsilon model was set to Realizable. Other important parameters of boundary conditions of two-dimensional CD nozzle stated in Fig. 5 are the lower horizontal straight-line is considered an axis line, the upper line as a wall, an initial vertical line is an inlet and the final vertical line is an outlet. However the wall we split into different categories such as base pressure, cavity, duct, and nozzle.
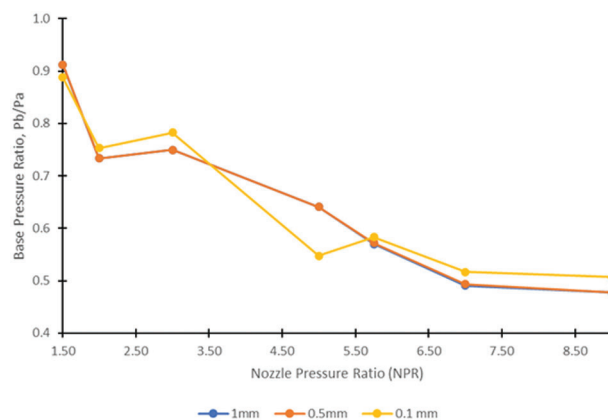
Figure 5: The base pressure for different element sizes having converged values

5 Results and Discussion

5.1 Mesh Independence Study

The mesh independence test has been carried out to find the optimum grid size. This is because, for higher NPR, more iterations are needed and higher computing time. Choosing a proper element size can obtain higher accuracy with less computing time. Generally, 10k iterations are enough for the solutions to

converge, but the iterations are set to 20k to ensure the solutions converge with high accuracy. The element size is changed several times to make sure the solution converges. The element size was 0.1 mm with nodes of about 50,353, and the number of elements, 49,594, was selected after a mesh independence check using three different element sizes, as displayed in Fig. 5.

5.2 Method Validation with Existing Work

NPR (P_{01}/P_a) was 2.10 chosen from the previous paper by Raymer [1] compared with the current work. This geometry validation aims to simulate the theoretical flow parameters by using CFD simulation (ANSYS Fluent) in 2D modelling for the model with cavity aspect ratio 1. The present work L/D was varied from 2 to 10 for validation (Fig. 6).
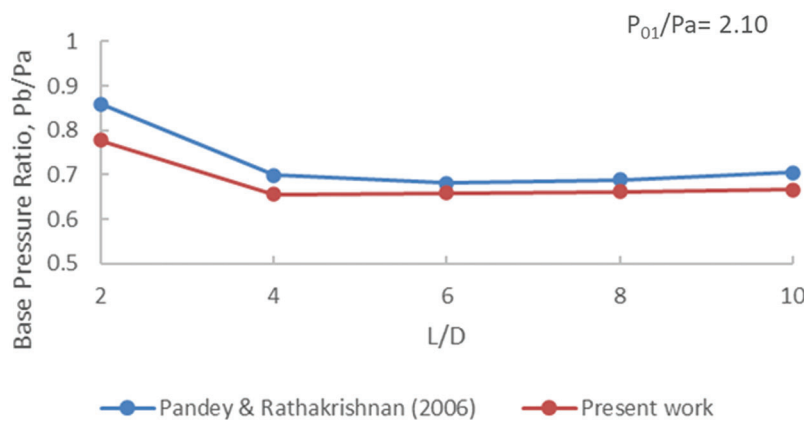
Figure 6: Verification of present work

The current and previous work data curves are represented in Fig. 6. The curves all have the same pattern, and each point is close to the next. Compared to the earlier work, the percentage error for the current simulation data is less than 10%. As a result, the validation of the present work was successful.

5.3 Base Pressure of Sudden Expansion Duct

The impact of the cavity and its geometry towards base pressure with the sudden increase in area for flow through nozzle flowing at supersonic Mach M = 1.8 are deliberated. The duct diameter is 16 mm, and the L/D varies, such as 1, 2, 3, 4, 6, 8, and 10. The NPRs chosen are 2, 3, 5, 5.75, 7, and 9. At these NPRs, initially, the flow remained overexpanded, later becomes correctly expanded at NPR = 5.75 and under-expanded at NPRs 7 and 9. The area ratio, NPR, and L/D influence the base pressure [30]. Further, Figs. 7a–7f explain the cavity geometry impact, expansion effect, and influence of the enlarged duct lengths. At lower NPRs, namely NPR = 2, 3, and 5, flow from the nozzle remains over-expanded and over-expansion levels at these NPRs are P_e/P_a = 0.35, 0.52, and 0.87. When nozzles are operated under the influence of an adverse pressure gradient, there will be an oblique shock at the nozzle exit, and the strength of the oblique shock will decrease with the progressive increase in the NPR. The impact of oblique shock at the nozzle exit is seen in the magnitude of the base pressure (Figs. 7a–7b). At NPR = 7, the over-expansion level has considerably decreased; hence, base pressure assumes low values in the absence of cavity. It is also seen that when duct length is L = 1D, it seems the flow did not attach to the duct wall, and its value is nearly equal to the ambient atmospheric value. Results show that at NPRs 2 and 5, control due to the cavity when placed at 1D location results in a considerable increase in the base pressure. However, at NPR = 3, the cavity decreases the base pressure. Additionally, observed that the cavity with ASR2 is not effective compared to ASR1.
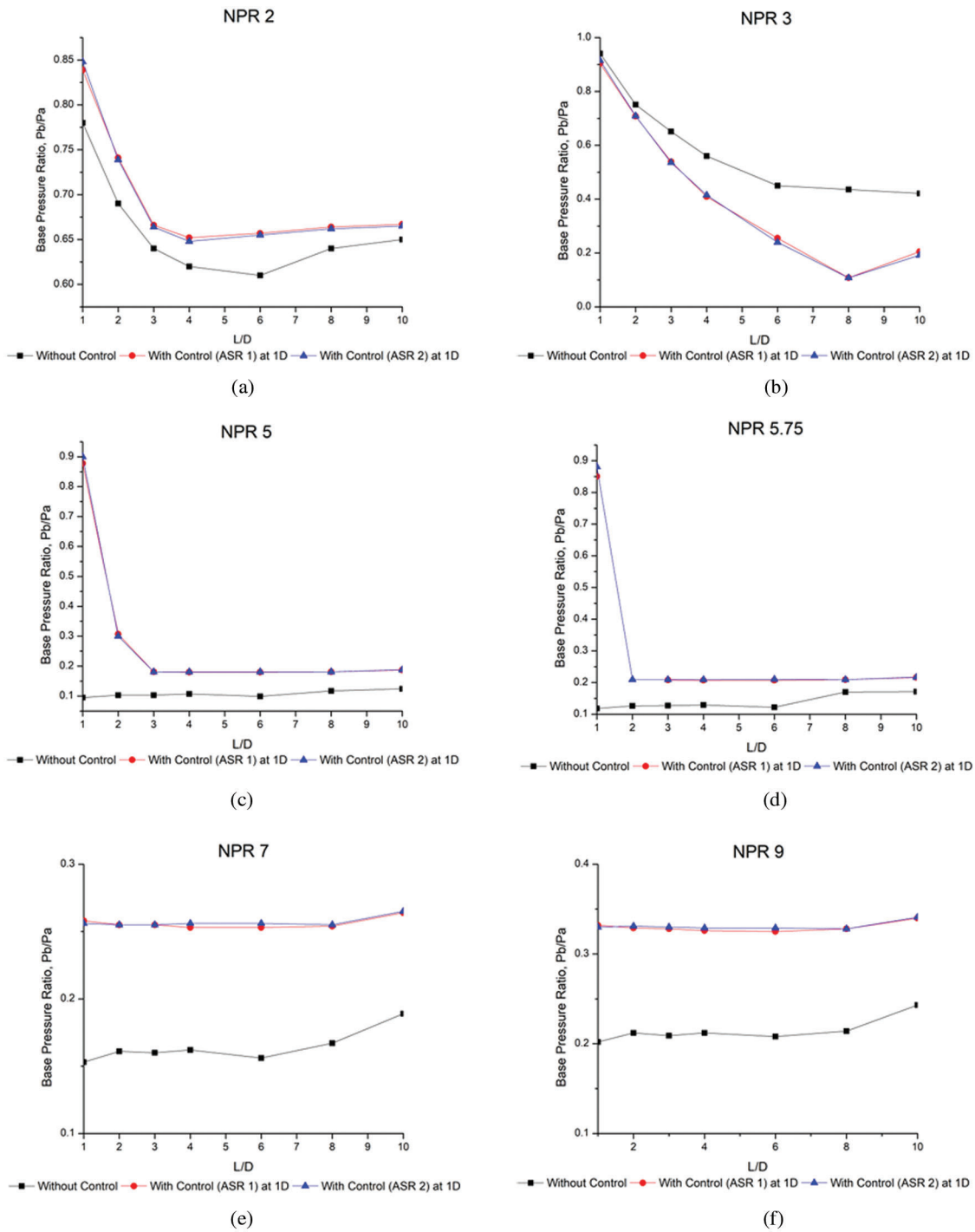
Figure 7: The base pressure ratio variation with L/D for plain duct and duct with control

For correctly expanded nozzles at NPR = 5.75 at Mach M = 1.8; ideally, the nozzle must be free from the waves (Fig. 7d). However, it is found that the Mach wave accompanies the flow. The flow pattern is similar to NPR = 5 as there is a marginal change in the level of expansion from 0. 87 to 1.0. For higher NPRs at 7 and 9, the flow is under-expanded. Whenever a control is used, whether active or passive, it is well known that it will become very effective when the nozzles are flowing under the influence of a favourable pressure gradient. An expansion fan is formed at the nozzle exit when jets are under-expanded. From Figs. 7e to 7f, it is seen that when the flow is under the influence of a favourable pressure gradient, control through cavities becomes effective, and there is a substantial increase in the base pressure seen.

Fig. 8 depicts the variation of the base pressure ratio with NPR. These results show that at lower duct lengths, L = 2D and 3D, the flow pattern is different due to the influence of the ambient pressure. In the absence of control, there is a continuous decline in the base pressure up to NPR = 5. There is a progressive increase in the base pressure. Passive flow management through the cavity is ineffective as long as the flow is over-expanded. It is also observed that the flow pattern is different duct lengths up to NPR = 5. It may be due to the combined effect of the shock interactions at these duct lengths, the impact of the ambient pressure, and the effect of the cavity size and locations. Once the flow is either correctly expanded or under-expanded, the control becomes efficient, and a considerable base pressure increases.

5.4 Flow Formation in CD Nozzle

As a contoured result, we have provided three different groups of results (Fig. 9). The group is determined by one set of parameters as follows:

1. L/D = 1, 2, 3, 4, 6, 8, and 10, Duct length = 16 mm, Cavity location from the base wall = 0.5D (6.5 mm), Cavity aspect ratio = 1, NPR = 5.
2. L/D = 2, 3, 4, 6, 8, and 10, Duct length = 32 mm, Cavity location from the base wall = 1D (14.5 mm), Cavity aspect ratio = 1, NPR = 5.
3. L//D = 2, 3, and 4, Duct length = 32 mm, Cavity location from the base wall = 1.5D (22.5 mm), Cavity aspect ratio = 1, NPR = 5.

As a result of contour, we have considered the static pressure in a CD nozzle for different parameters. The flow field varies based on the parameters, and if the duct length is long, the flow formation is lower in the rear part of the sudden expansion duct. The recirculation zone will form inside the cavity when the cavity controls the flow, and the pressure rate is meagre. However, convergent duct, the pressure is high when it reaches the throat; it has a sudden reduction and continuously decreases the divergent part of the nozzle. Moreover, at sudden expansion, duct nozzle exit produces drag in the base of the duct, which may result in an increased base drag. For the reduction of base drag and recirculation zone, the cavities can absorb the recirculated flow, which may increase the forward flow rate of the sudden expansion duct to increase the exit pressure to increase the thrust in the nozzle for high-speed flow vehicles. This research has been shown by the two-dimensional finite volume method of CD nozzle, and Fig. 9 shows a contour of static pressure for the same NPR at different L/D and duct diameters.
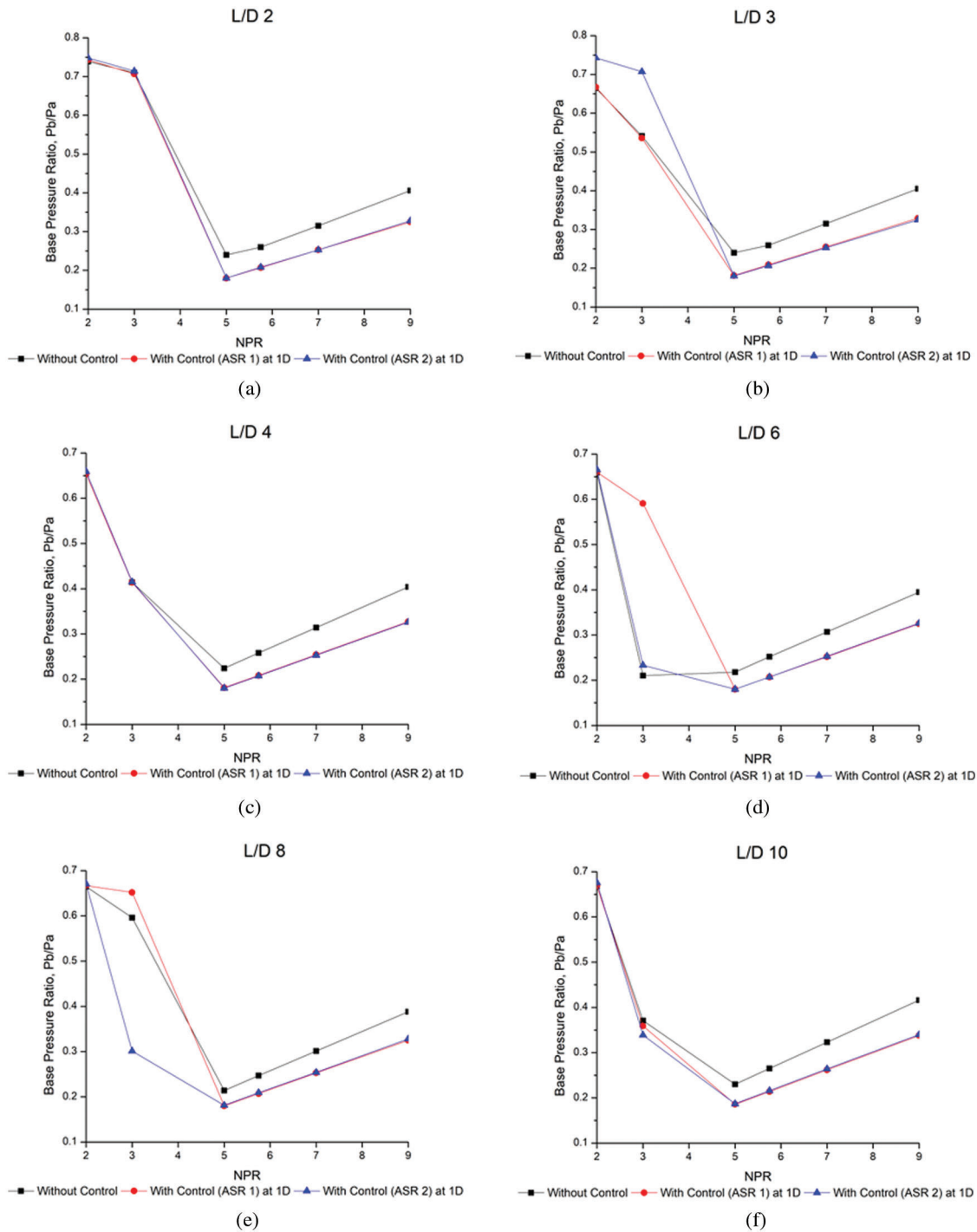
Figure 8: The base pressure ratio variation with NPR for plain duct and duct with control
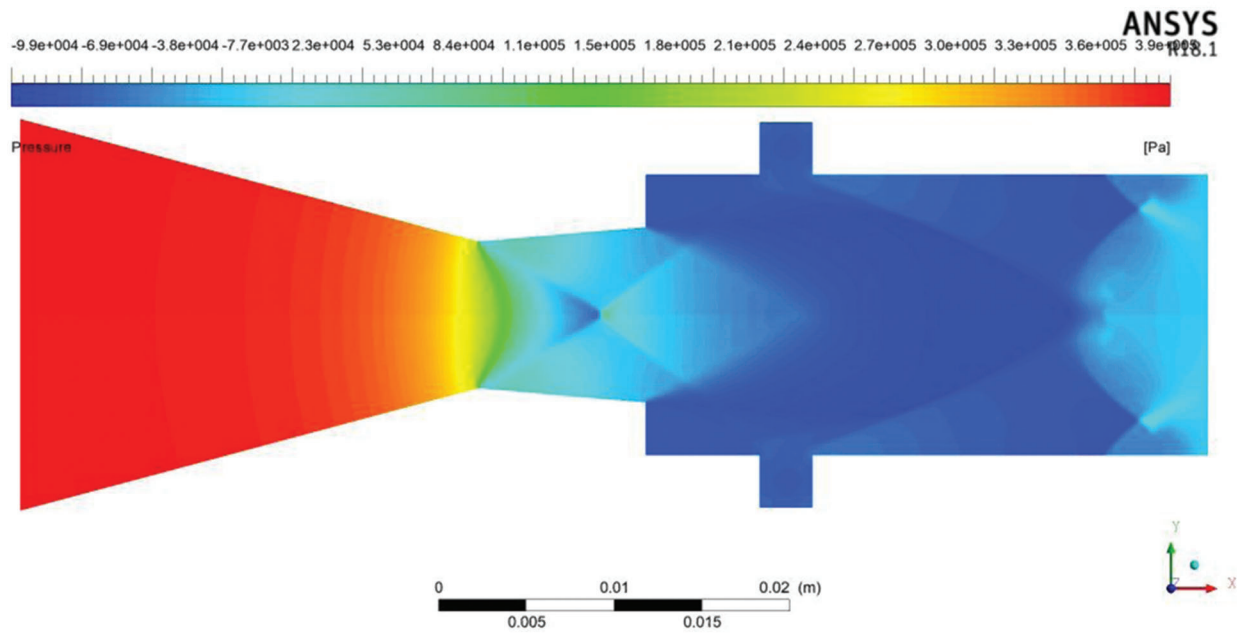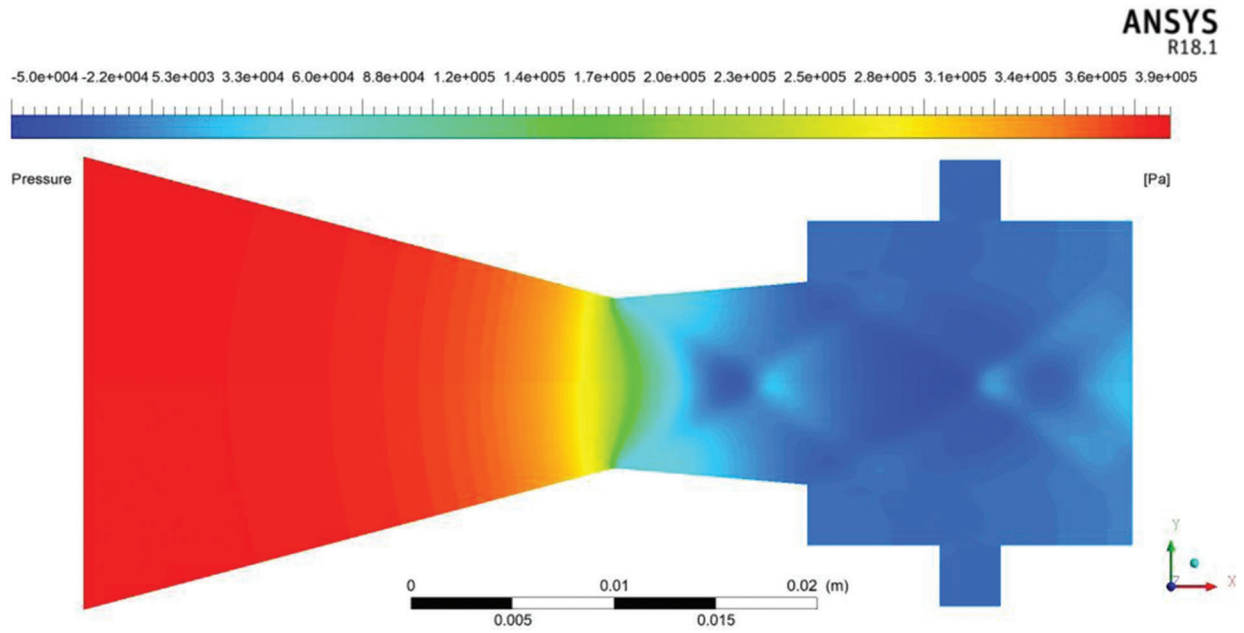
Figure 9: (Continued)
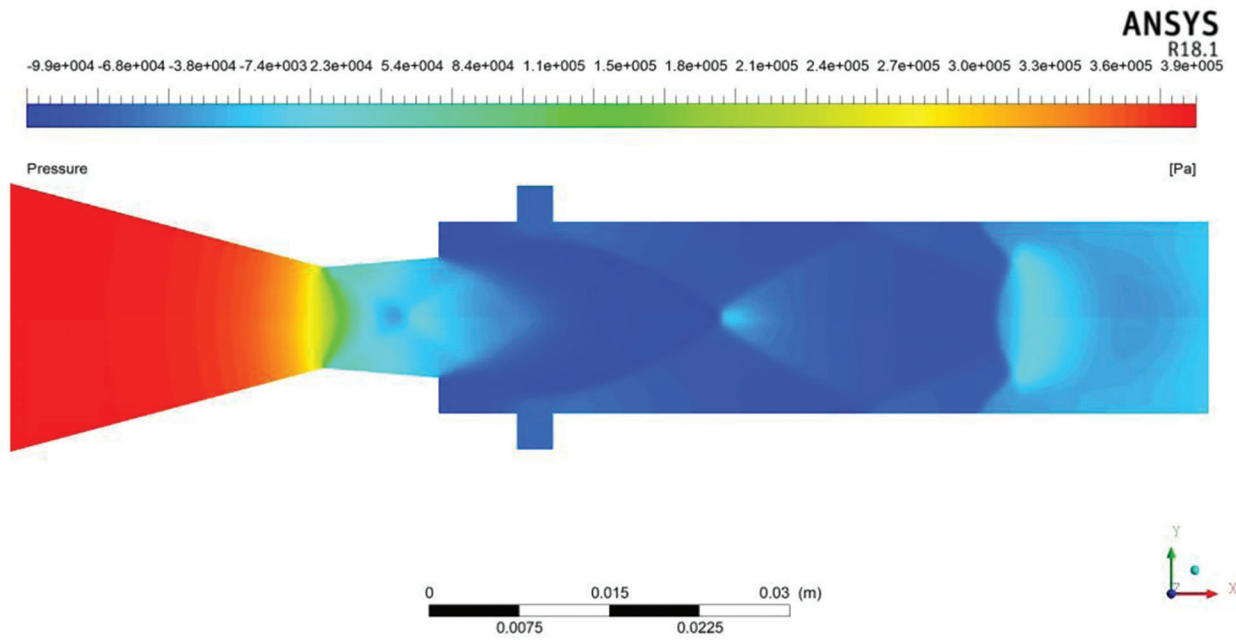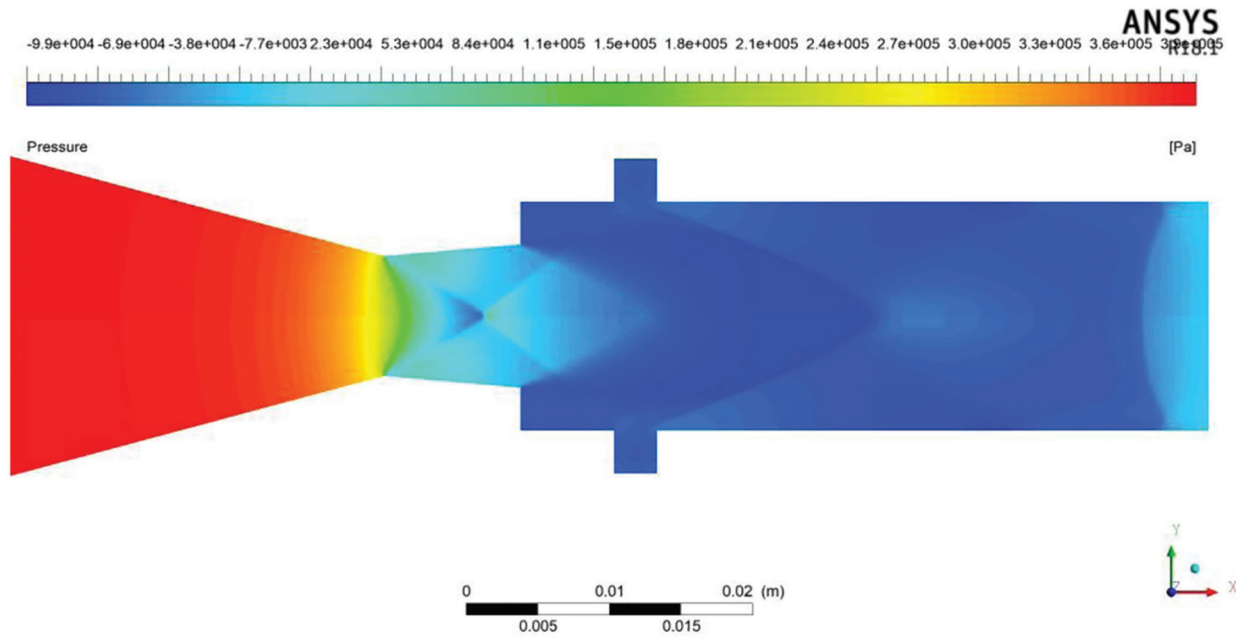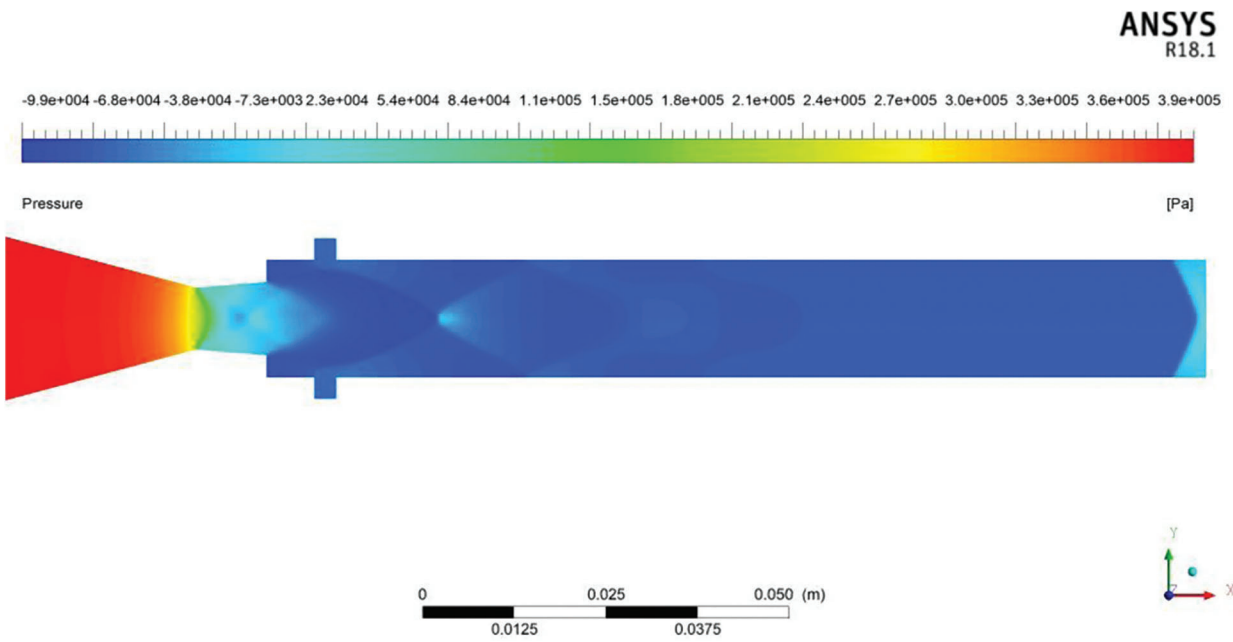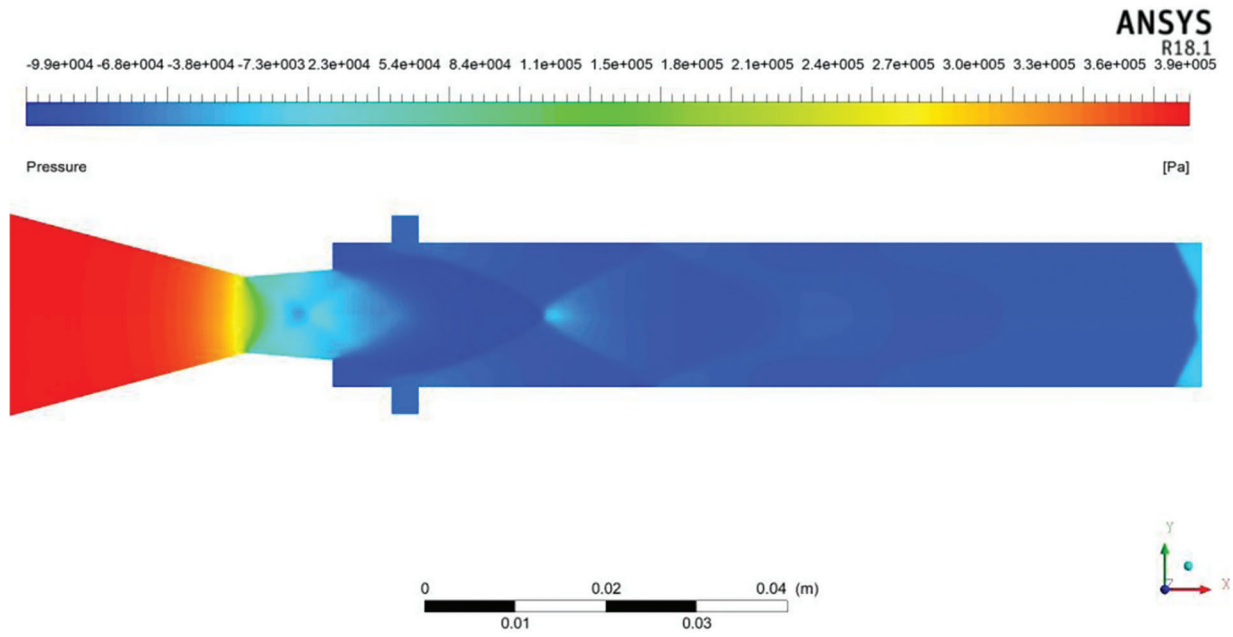
**Figure 9:** (Continued)
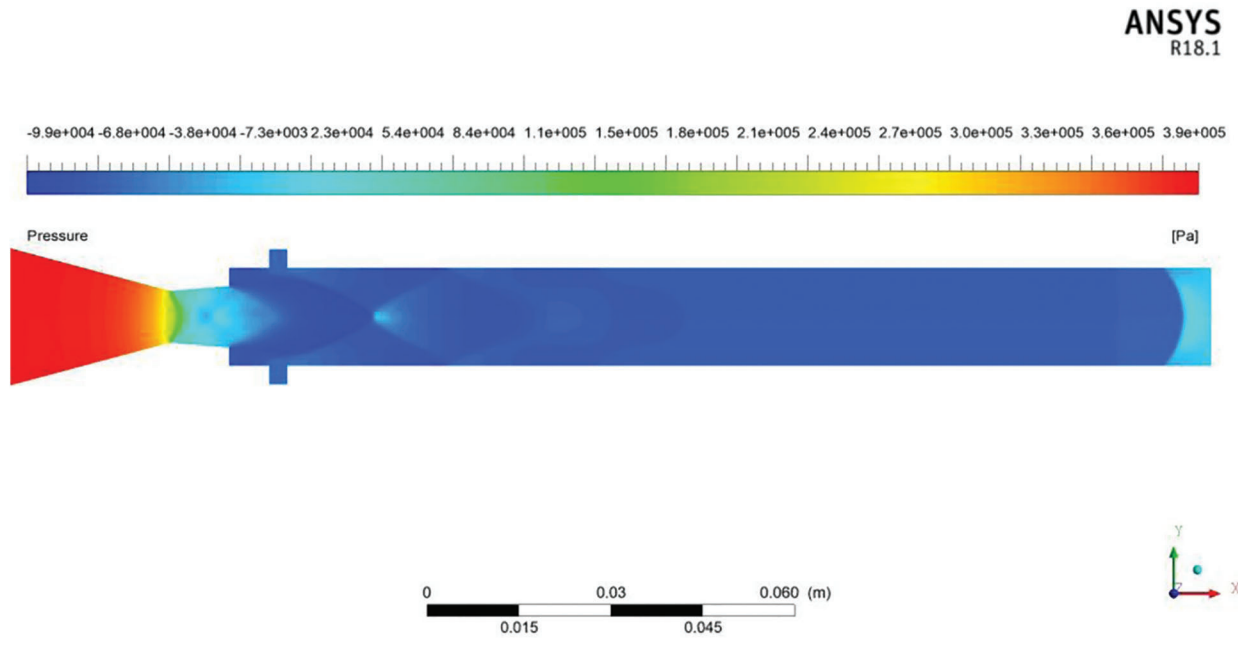
Figure 9: (Continued)

(Group 1)
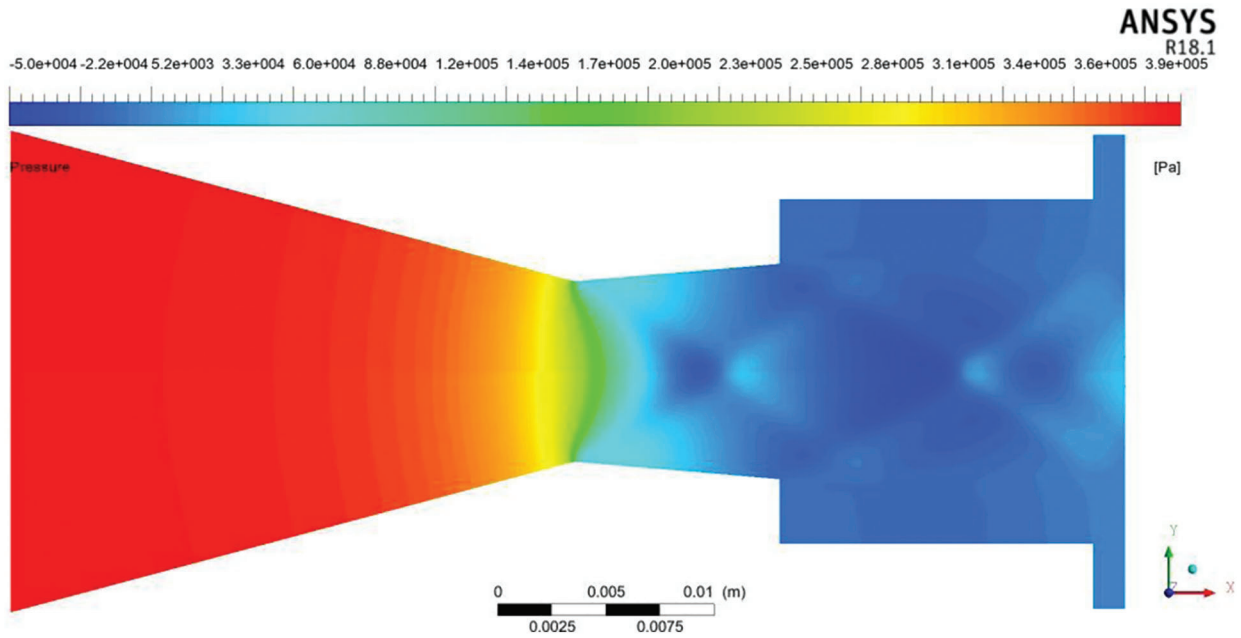
**Figure 9:** (Continued)
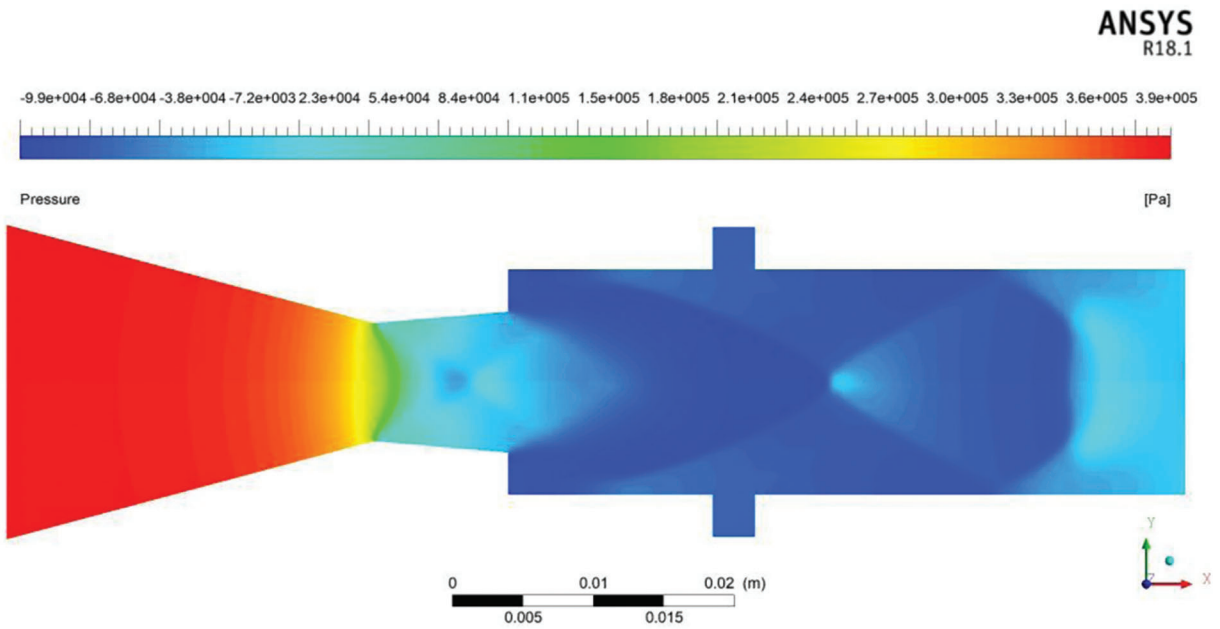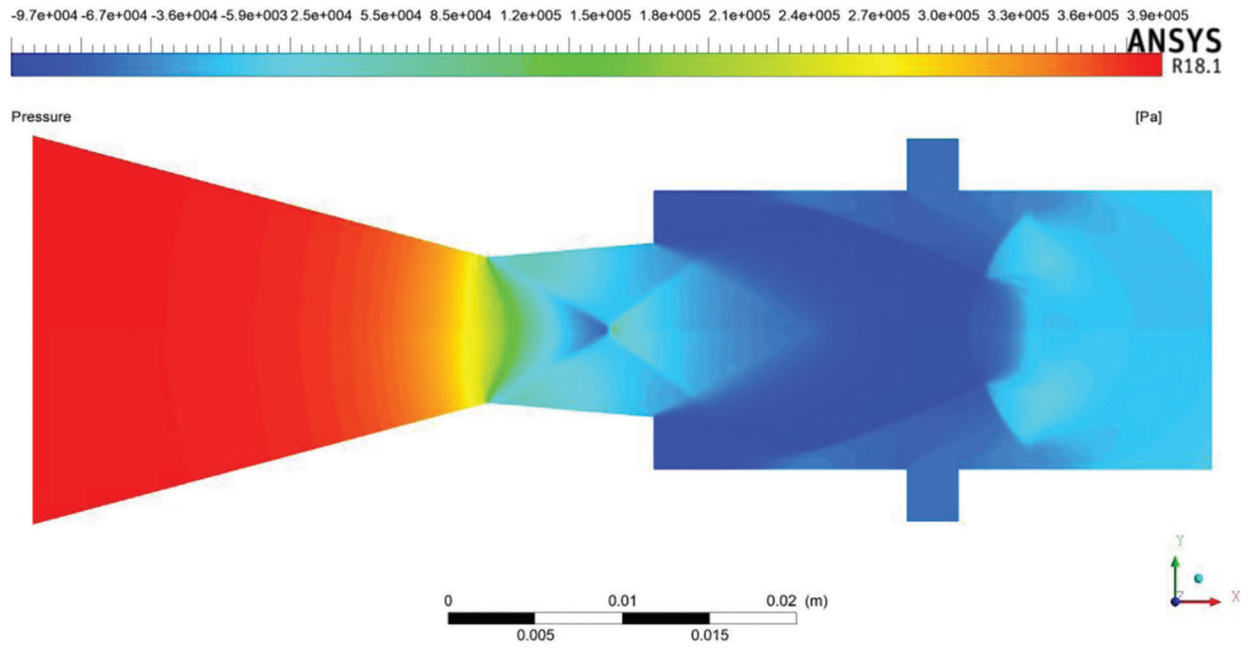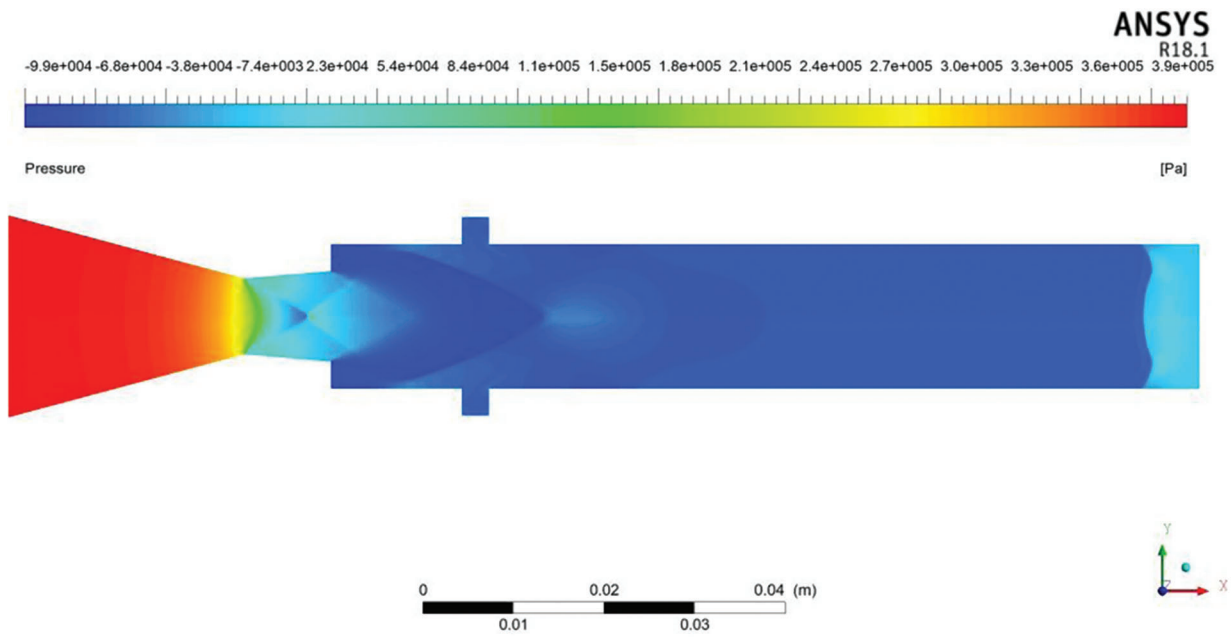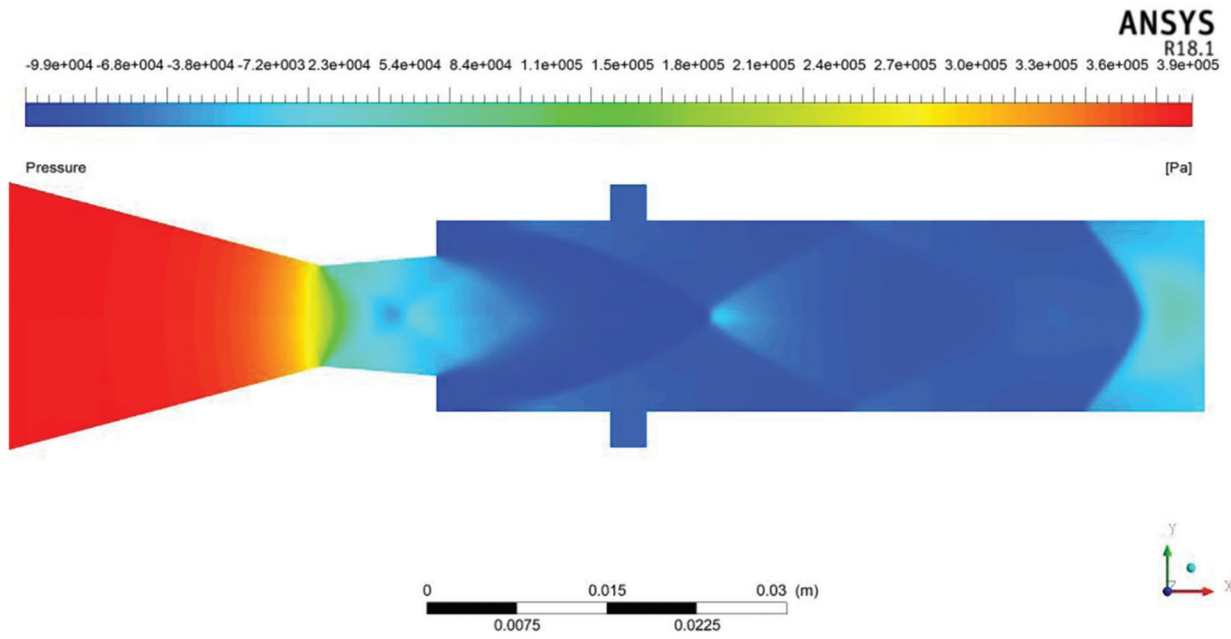
Figure 9: (Continued)
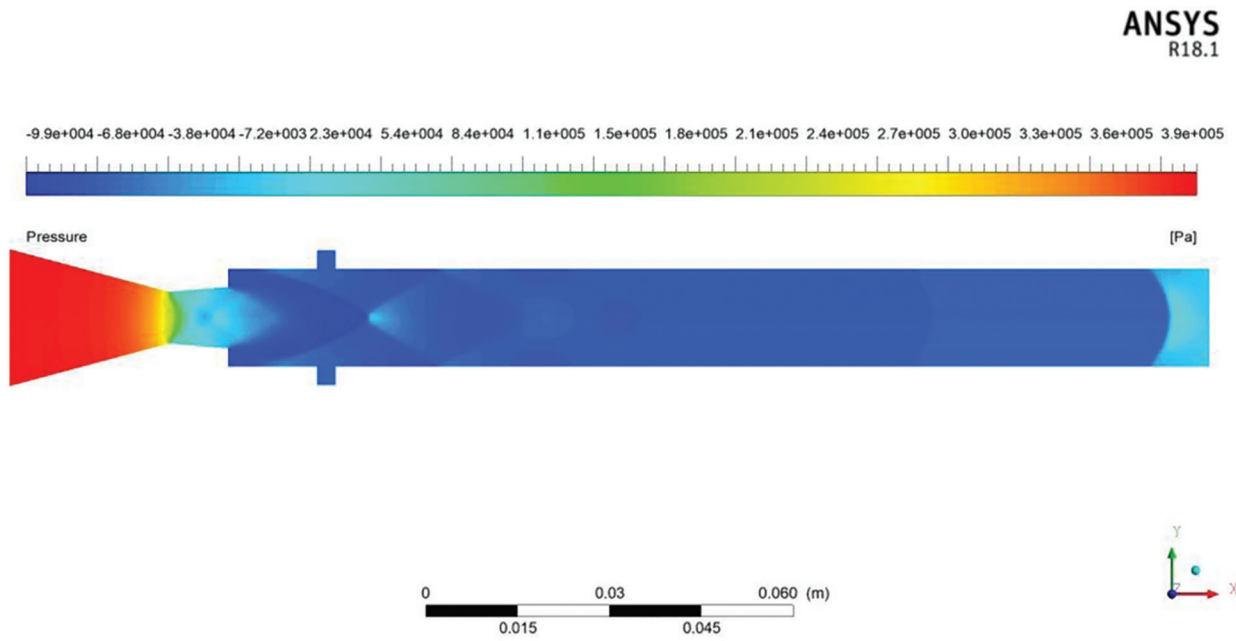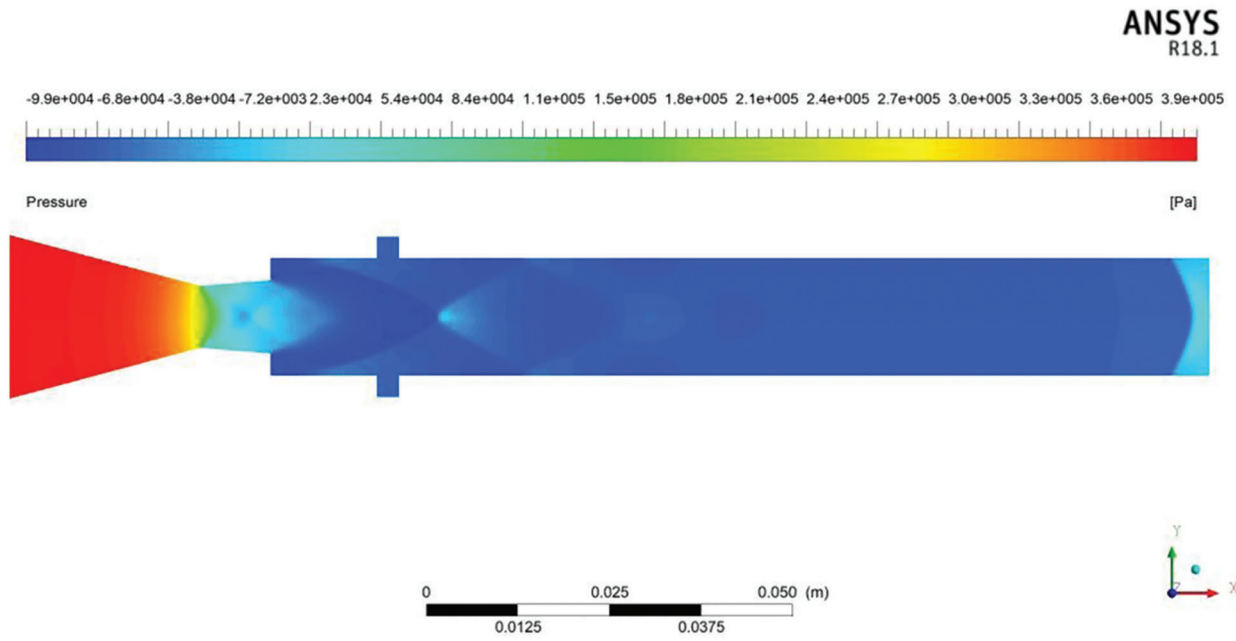
Figure 9: (Continued)

(Group 2)

Figure 9: (Continued)
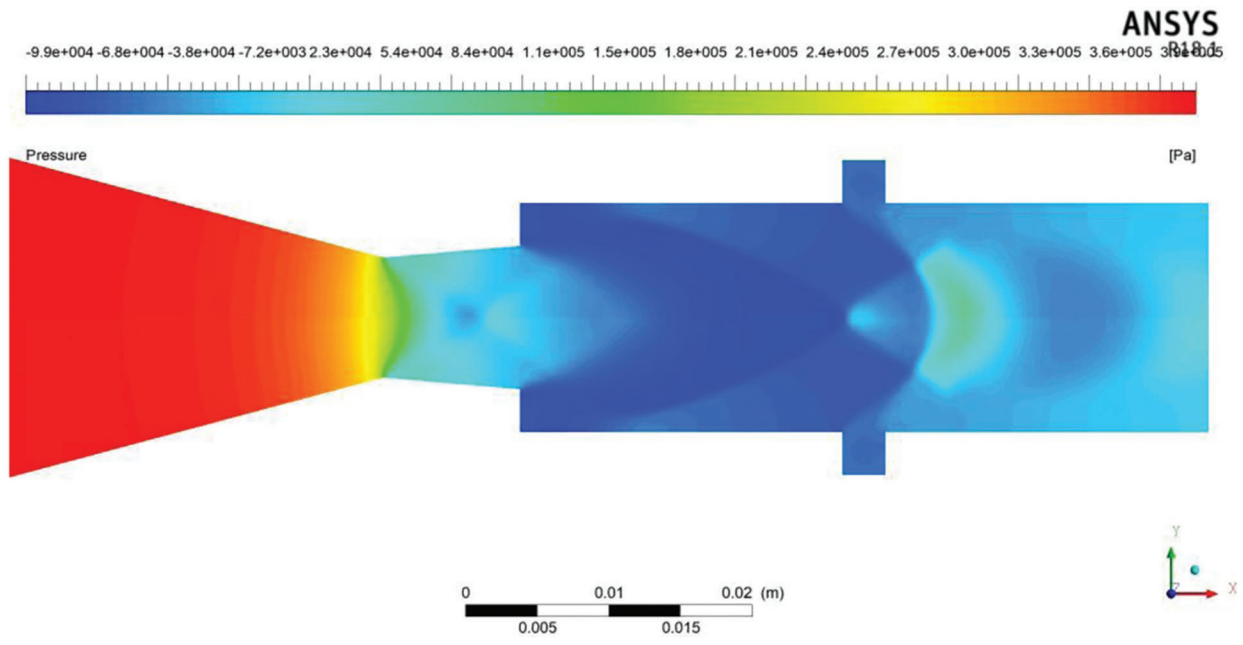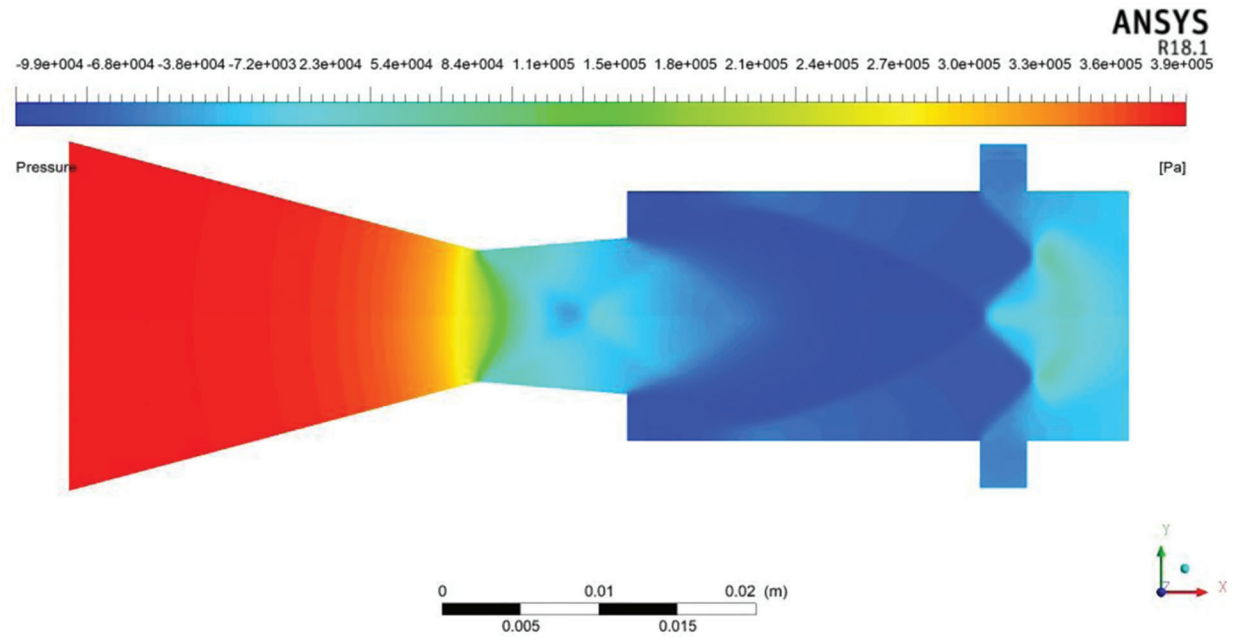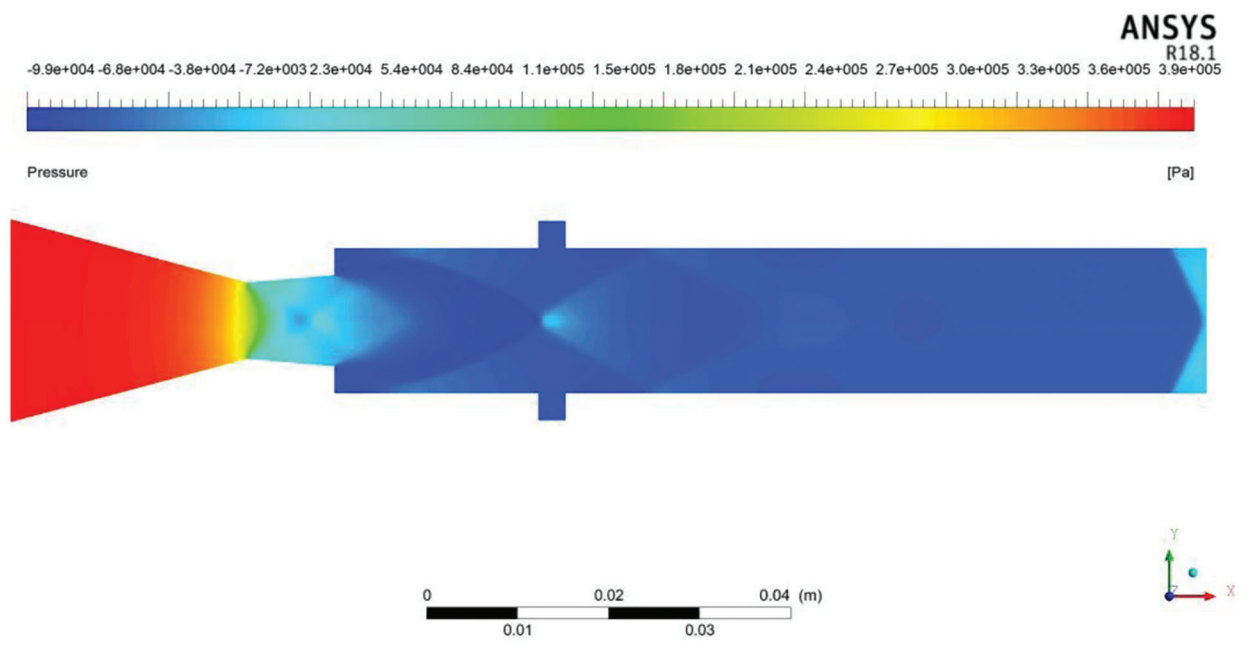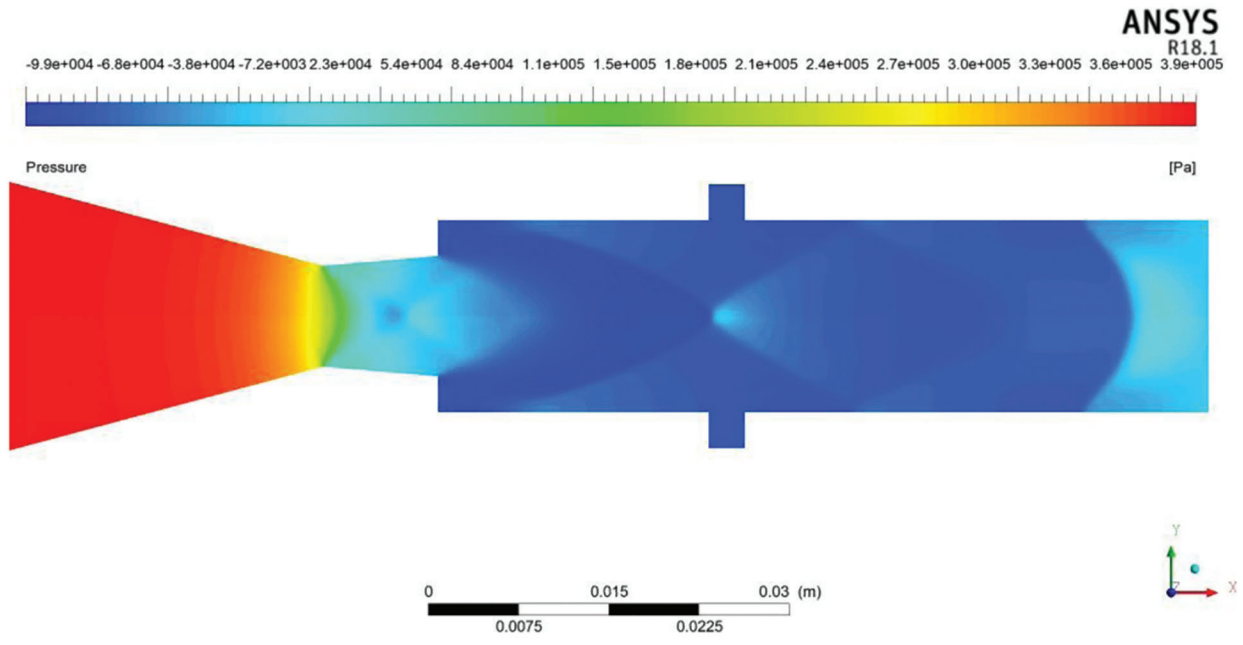
Figure 9: (Continued)

Figure 9: (Continued)
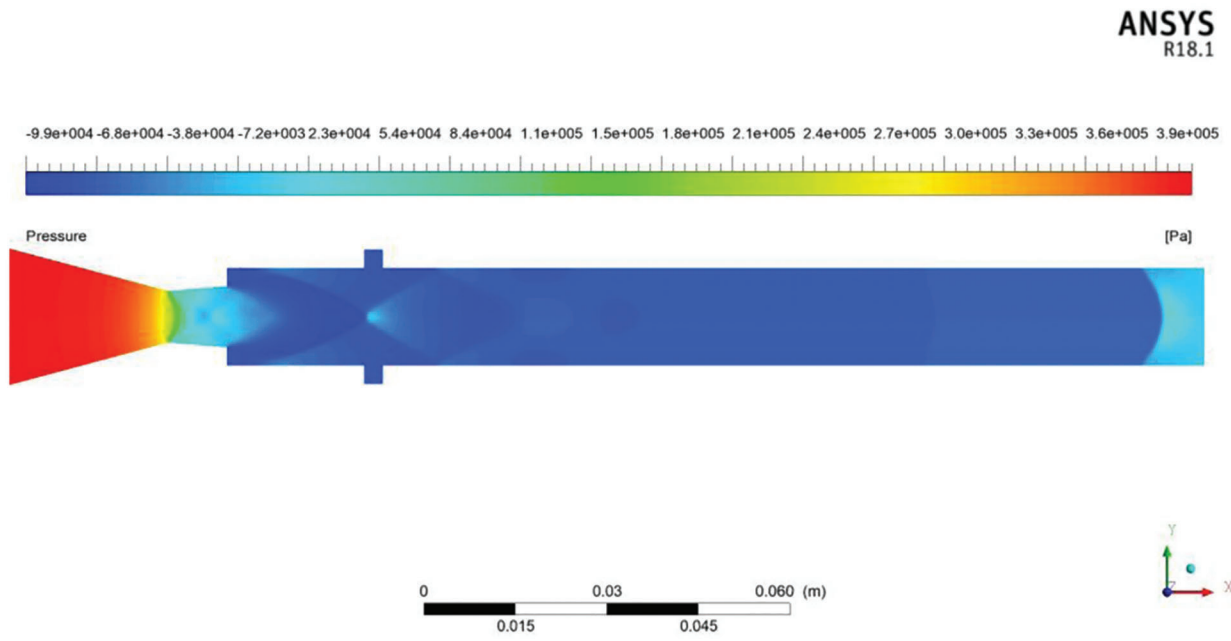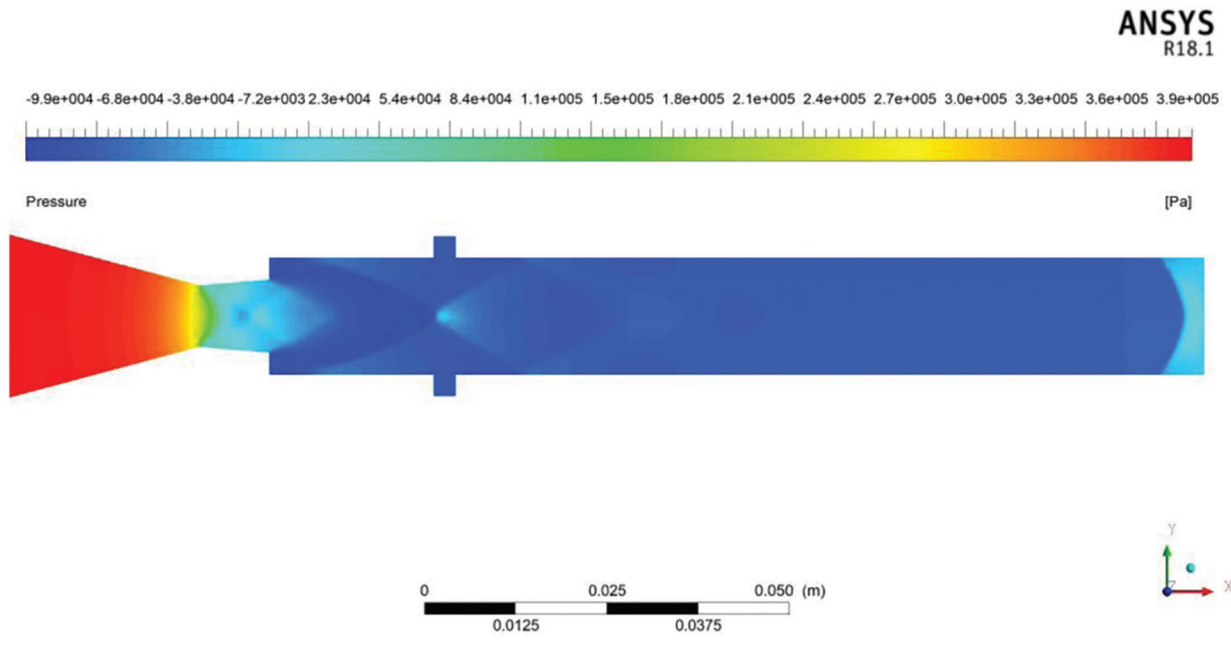
(Group 3)

Figure 9: Flow field in different L/D for NPR 5

6 Conclusion

In conclusion, in this study, the passive control effectiveness in the cavity to regulate the base pressure is demonstrated. The cavity in the duct influenced the base pressure at Mach number 1.8 and the area ratio of 2.56. The control becomes effective once the nozzles are correctly expanded or under-expanded. Any increase in the cavity size is insignificant and does not result in a significant rise in the base pressure. The pressure contours at different NPR and L/D are studied and illustrated in detail, which will be very useful for a better understanding of the pressure variations in the nozzle and the duct. Compared to a plain tube, the presence of a cavity at the duct significantly impacts the base pressure. Increasing the cavity aspect ratio, on the other hand, does not affect the pressure in the wake. We increased the height of the cavity in this study. However, increasing the cavity width will affect the pressure in the separated region because the changed cavity width may fall within the reattachment length and impact the base flow field.

Conflicts of Interest: The authors declare that they have no conflicts of interest to report regarding the present study.

References

1. Raymer, D. P. (2018). *Aircraft design: A conceptual approach (AIAA Education) (AIAA Education Series)*. 6th edition. American Institute of Aeronautics & Ast.

2. Wick, R. S. (1953). The effect of boundary layer on sonic flow through an abrupt cross-sectional area change. *Journal of the Aeronautical Sciences, 20(10),* 675–682. DOI 10.2514/8.2794.

3. Pandey, K., Rathakrishnan, E. (2006). Annular cavities for base flow control. *International Journal of Turbo and Jet Engines, 23(2)*, 113–128. DOI 10.1515/tjj.2006.23.2.113.

4. Nusselt, W. (1929). Heat dissipation from horizontal tubes and wires to gases and liquids. *Ver DeutIng, 73,* 1475–1478.

5. Korst, H. (1956). A theory of base pressure in transonic and supersonic flow. *Journal of Applied Mechanics, 23(4),* 593–600. DOI 10.1115/1.4011405.

6. Anderson, J. S., Williams, T. J. (1968). Base pressure and noise produced by the abrupt expansion of air in a cylindrical duct. *Journal of Mechanical Engineering Science, 10(3),* 262–268. DOI 10.1243/JMES_JOUR_1968_010_038_02.

7. Srikanth, R., Rathakrishnan, E. (1991). Flow-through pipes with sudden enlargement. *Mechanics Research Communications, 18(4),* 199–206. DOI 10.1016/0093-6413(91)90067-7.

8. Asadullah, M., Khan, S. A., Soudagar, M. E. M., Vaishak, T. R. (2019). A comparison of the effect of single and multiple cavities on base flows. *2018 IEEE 5th International Conference on Engineering Technologies & Applied Sciences*, Bangkok, Thailand.

9. Tanner, M. (1988). The base cavity at angles of incidence. *AIAA Journal, 26(3),* 376–377. DOI 10.2514/3.9903.

10. Viswanath, P. R., Patil, S. R. (1990). Effectiveness of passive devices for axisymmetric base drag reduction at Mach 2. *Journal of Spacecraft and Rockets, 27(3),* 234–237. DOI 10.2514/3.26130.

11. Viswanath, P. R. (1994). *Base drag characteristics of multi-step afterbodies*. Bangalore, Indien, Report NAL PD EA, 9507.

12. Viswanath, P. R. (1996). Flow management techniques for base and afterbody drag reduction. *Progress in Aerospace Sciences, 32(2–3),* 79–129. DOI 10.1016/0376-0421(95)00003-8.

13. Mair, W. A. (1965). The effect of a rear-mounted disc on the drag of a blunt-based body of revolution. *The Aeronautical Journal, 16,* 350–360. DOI 10.1017/S0001925900003589.

14. Rathakrishnan, E. (1999). Effect of splitter plate on bluff body drag. *AIAA Journal, 37(9),* 1125–1126. DOI 10.2514/2.823.

15. Rathakrishnan, E. (2001). Effect of ribs on suddenly expanded flows. *AIAA Journal, 39(7),* 1402–1404. DOI 10.2514/2.1461.

16. Khan, S. A., Mokashi, I., Aabid, A., Faheem, M. (2019). Experimental research on wall pressure distribution in CD nozzle at Mach number 1.1 for area ratio 3.24. *International Journal of Recent Technology and Engineering, 8(2S3),* 971–975. DOI 10.35940/ijrte.B1182.0782S319.

17. Aabid, A., Afghan Khan, S. (2021). Determination of wall pressure flows at supersonic mach numbers. *Materials Today: Proceedings, 38,* 2347–2352. DOI 10.1016/j.matpr.2020.06.538.

18. Aabid, A., Khan, S. A. (2021). Studies on flows development in a suddenly expanded circular duct at supersonic mach numbers. *International Journal of Heat and Technology, 39(1),* 185–194.

19. Aabid, A., Khan, S. A. (2021). Investigation of high-speed flow control from CD nozzle using design of experiments and CFD methods. *Arabian Journal for Science and Engineering, 46(3),* 2201–2230. DOI 10.1007/s13369-020-05042-z.

20. Afghan, S., Mohamed, O., Aabid, A. (2021). CFD analysis of compressible flows in a convergent-divergent nozzle. *Materials Today: Proceedings, 46,* 2835–2842. DOI 10.1016/j.matpr.2021.03.074.

21. Khan, S. A., Aabid, A., Ghasi, F. A. M., Al-Robaian, A. A., Alsagri, S. A. (2019). Analysis of area ratio in a CD nozzle with suddenly expanded duct using CFD method. *CFD Letters, 11(5),* 61–71.

22. Aabid, A., Afghan Khan, S., Baig, M. (2022). Numerical analysis of a microjet-based method for active flow control in convergent-divergent nozzles with a sudden expansion duct. *Fluid Dynamics & Materials Processing, 18(6),* 1877–1900. DOI 10.32604/fdmp.2022.021860.

23. Aabid, A., Khan, S. A., Afzal, A., Baig, M. (2021). Investigation of tiny jet locations effect in a sudden expansion duct for high-speed flows control using experimental and optimization methods. *Meccanica, 57,* 17–42. DOI 10.1007/s11012-021-01449-6.

24. Al-khalifah, T., Aabid, A., Khan, S. A., Azami Bin, M. H., Baig, M. (2021). Response surface analysis of the nozzle flow parameters at supersonic flow through microjets. *Australian Journal of Mechanical Engineering, 13(2),* 1–15. DOI 10.1080/14484846.2021.1938954.

25. Quadros, J. D., Khan, S. A., Aabid, A., Alam, M. S., Baig, M. (2021). Machine learning applications in modelling and analysis of base pressure in suddenly expanded flows. *Aerospace, 8(11),* 318. DOI 10.3390/aerospace8110318.

26. Aabid, A., Khan, S. A., Baig, M. (2021). A critical review of supersonic flow control for high-speed applications. *Applied Sciences, 11(15),* 6899. DOI 10.3390/app11156899.

27. Pushpa, B. V., Sankar, M., Mebarek-Oudina, F. (2021). Buoyant convective flow and heat dissipation of Cu–H_2O nanoliquids in an annulus through a thin baffle. *Journal of Nanofluids, 10(2),* 292–304. DOI 10.1166/jon.2021.1782.

28. Marzougui, S., Mebarek-Oudina, F., Magherbi, M., Mchirgui, A. (2021). Entropy generation and heat transport of Cu–water nanoliquid in porous lid-driven cavity through magnetic field. *International Journal of Numerical Methods for Heat & Fluid Flow.* DOI 10.1108/HFF-04-2021-0288.

29. Koomullil, R., Soni, B., Singh, R. (2008a). A comprehensive generalized mesh system for CFD applications. *Mathematics and Computers in Simulation, 78(5–6),* 605–617. DOI 10.1016/j.matcom.2008.04.005.

30. Khan, S. A., Asadullah, M. (2018). Passive control of base drag in compressible subsonic flow using multiple cavity. *International Journal of Mechanical and Production Engineering Research and Development (IJMPERD), 8(4),* 39–44. DOI 10.24247/ijmperdaug20185.